Theoretical and Applied Climatology
https://doi.org/10.1007/s00704-023-04407-2

ORIGINAL PAPER

Unraveling diurnal asymmetry of surface temperature under warming scenarios in diverse agroclimate zones of India

Nidhi Singh[1,2] · Manisha Chaturvedi[1] · R. K. Mall[1]

Received: 14 April 2022 / Accepted: 18 February 2023

Abstract
Diurnal temperature range (DTR) which reflects the difference between the daily maximum (Tmax) and minimum temperature (Tmin) is an important indication of changing climate and a critical thermal metric to assess the impact on agriculture, biodiversity, water resources, and human health. The major aim of this study is to assess the probable future spatio-temporal changes in the Tmax, Tmin, and DTR and their long-term warming trend from 2006 to 2099 under two representative concentration pathways (hereafter RCP4.5 and RCP8.5) over diverse agroclimatic regions of India. The observed data from India Meteorological Department (IMD) was used to evaluate the performance of climate models (1970–2005). The result shows a very slight underestimation in DTR by models compared to the observed. In future projections, we found a reduction in DTR (0.001 to 0.020 °C/year) partly linked to the substantial increase in Tmin (0.020 to 0.071 °C/year) than Tmax (0.031 to 0.060 °C/year) that was stronger in far twenty-first-century future under RCP8.5. The decline in DTR was profound and consistent over northern India (up to 3 °C) surrounding the Indo-Gangetic Plain, western dry region, and part of central India with the highest decline observed in winter and pre-monsoon season. However, a decline in DTR was also anticipated over the plateau, coastal, and eastern Himalayas region. Change in land use land cover (LULC) also complimented the decline in DTR. The main findings of the study advocate implementation of a robust framework for climate change adaptation strategies to mitigate adverse consequences to the natural ecosystem and human health over specific regions arising due to declining DTR.

1 Introduction

There is evidence that DTR could provide more particulars about climate change research than the mean average temperature (Tmean) and clarity about human-centric induced climate change (Wang et al. 2014; Lindvall and Svensson 2015). At a global level, the rise in the rate of Tmin has been much faster than Tmax subsequently causing DTR to decrease (Karl et al. 1991, 1993; Hua and Chen 2013; Lindvall and Svensson 2015; He et al. 2015). For example, past observational studies reported a global decrease in DTR by 0.07 °C/decade during 1950–1980 (Vose et al. 2005) to 0.036 °C/decade between 1901 and 2014 with a relatively smaller increase in the Tmax (1.1 °C) as compared to the Tmin (1.6 °C) (Sun et al. 2019). However, there have been regional inconsistencies such as in the mid-latitudes and low-latitude regions like East Asia, the decrease in DTR is mainly attributed to a reduction in daily Tmax, whereas in India, the decline in DTR is mainly due to the increase in daily Tmin (Hua and Chen 2013; Vinnarasi et al. 2017; Waqas and Athar 2018; Mall et al. 2021; IPCC 2021).

The warming is likely to have serious repercussions on cloud cover, accelerating extreme heat wave events, droughts, intense rainfall and flooding, wildfires, tropical cyclones, and melting of ice (Cox et al. 2020; Mall et al. 2019). These adverse events will directly or indirectly be linked to loss of agricultural production, erratic changes in water resources, adverse health effects and further loss of livelihood, and food security issues (Mall et al. 2018, 2021; Bhatt et al. 2019; Singh et al. 2019; Sonkar et al. 2019; Sonkar et al. 2020; Singh et al. 2021a, b; Patel et al. 2022; Jaiswal et al. 2023; Rajput et al. 2023; Dubey et al. 2023).

Moreover, DTR could be influenced by several processes. Aerosols and their interaction with clouds (cloud cover), greenhouse emissions and humidity, and land surface characteristics (LULC) influence DTR in multiple ways, such

✉ R. K. Mall
mall_raj@rediffmail.com

[1] DST-Mahamana Centre of Excellence in Climate Change Research, Institute of Environment and Sustainable Development, Banaras Hindu University, Varanasi, India

[2] Leibniz Research Institute for Environmental Medicine (IUF), Düsseldorf, Germany

Published online: 03 March 2023

as by the fraction of solar energy absorbed by the surface albedo, by modulating the changes in canopy evaporation and transpiration and the evaporative cooling by the soil moisture (Dai et al. 1999; Hua et al. 2013; Lindvall and Svensson 2015).

Simulation of future changes in DTR could provide valuable information as they provide vital scientific information to combat climate change and effectively manage the associated impacts. However, past studies reported the inefficiency of general circulation models (GCMs) to capture the magnitude of change in DTR (Stone and Weaver 2002; Braganza et al. 2004; Dai and Trenberth 2004; Lobell et al. 2007; Wild 2009; Zhou et al. 2010; Lewis and Karoly 2013; Sillmann et al. 2013). Several studies reported different factors to cause the incompetency of a model to simulate DTR efficiently, such as the poor representation of the stable planetary boundary layer (McNider et al. 2012), modeling of clouds, and aerosols, surface solar radiation (Srad) and soil moisture that could also cause large intermodel discrepancies (Wild 2009; Fischer et al. 2012; Sillmann et al. 2013; Cubasch et al. 2013; Lindvall and Svensson 2015; Cattiaux et al. 2015). Our lack of understanding of different atmospheric processes also leads to deviation of model outputs from the actual scenarios. Therefore, reliance on one simulation model would be inadequate to quantify the uncertainty in future changes in DTR.

Despite being an important factor to assess climate change acceleration, only a handful of studies have discussed the past and future changes in the spatiotemporal trend of DTR and its impact (Ullah et al. 2018; Salehnia et al. 2020). The high asymmetry in DTR depending upon spatial and temporal trends and an active monsoon pattern makes India different from the other parts of the world. A recent study on past annual and seasonal trends in the DTR over 14 different agroclimatic regions of India showed a decreasing trend in DTR (0.02 °C/decade) after 1991 owing to a distinct increase in Tmin (0.210 °C/decade) than Tmax (Mall et al. 2021). Similarly, Vinnarasi et al. (2017) reported a decrease in DTR up to 2 °C in some parts of India. It was found that regions of south India that usually witness low DTR have shown an increasing trend in DTR, whereas regions of north India characterized by high DTR were showing a declining trend. This past evidence demands the assessment of the causes of these profound spatiotemporal heterogeneity and changes in future.

Acknowledging the above research gap, we base our analysis on climate simulations provided by modeling 5 GCM groups participating in the Fifth Phase of the Coupled Model Intercomparison Project (CMIP5) into respective RCMs along with the other RCM, i.e., RegCM4. The analysis was performed over 14 agroclimatic zones of India. This paper aims to document the past (1970–2005) and projected changes in DTR, Tmax, and Tmin at annual and seasonal levels with the associated uncertainties for the two RCP scenarios RCP4.5 and RCP8.5 in two future periods: mid-century (2041–2060) and far-century (2071–2099). The role of LULC in the projected changes in DTR, Tmax, and Tmin was also analyzed. The role of Srad, cloud cover, and aerosols were also incorporated from other literature sources over the same study region. Study area, data, methods, and computation of indices are described in "Section 2," result and discussion in "Section 3," and conclusions are drawn in "Section 4."

2 Material and methods

2.1 Study area

The present study considers India as a whole divided into 14 different agroclimatic zones based on physiography, cropping patterns, climate, and soil type (Mall et al. 2021). The geographical location and topographical characteristics of the study area are shown in Fig. 1. An additional zone that lies outside (island) of the mainland is not considered in the present study. The climate type of India is mainly tropical monsoon with large regional variations in terms of rainfall, temperature, and vegetation type. There are four distinct seasons in India, winter (January–February: JF), pre-monsoon (March–April-May: MAM), monsoon (June-July–August-September: JJAS), and post-monsoon (October–November-December: OND) (https://www.imdpune.gov.in/Weather/Reports/glossary.pdf). A distinct cold spell during winter and hot and dry heatwave (referred to as Loo) in summer are prominent in the northern part of the country. A persistent thick aerosol layer characterizes entire India with a heavy aerosol loading found above the Indo-Gangetic Plain (IGP) in the northern part of India (Dey and Di Girolamo 2011; Kumar et al. 2018; Singh et al. 2021c), which is also the most productive region of India (Sonkar et al. 2019). Therefore, IGP often remains the center of investigation.

2.2 Data

The daily data on Tmax and Tmin for the historical and future periods was collected as outputs from six dynamically downscaled climate projections (Table S1). DTR was defined as the difference between the daily Tmax and daily Tmin. The model datasets comprise five dynamically downscaled projections using a high-resolution RCM "Conformal Cubic Atmospheric Model" (CCAM) developed at Commonwealth Scientific and Industrial Research Organization (CSIRO) Australia driven from five different GCMs, namely, ACCESS 1.0, CNRM-CM5, MPI-ESM-LR, NorESM-1 M, and GFDL-CM3. The other RCM, i.e., RegCM4 (downscaled using parent GCM "LMDZ,"

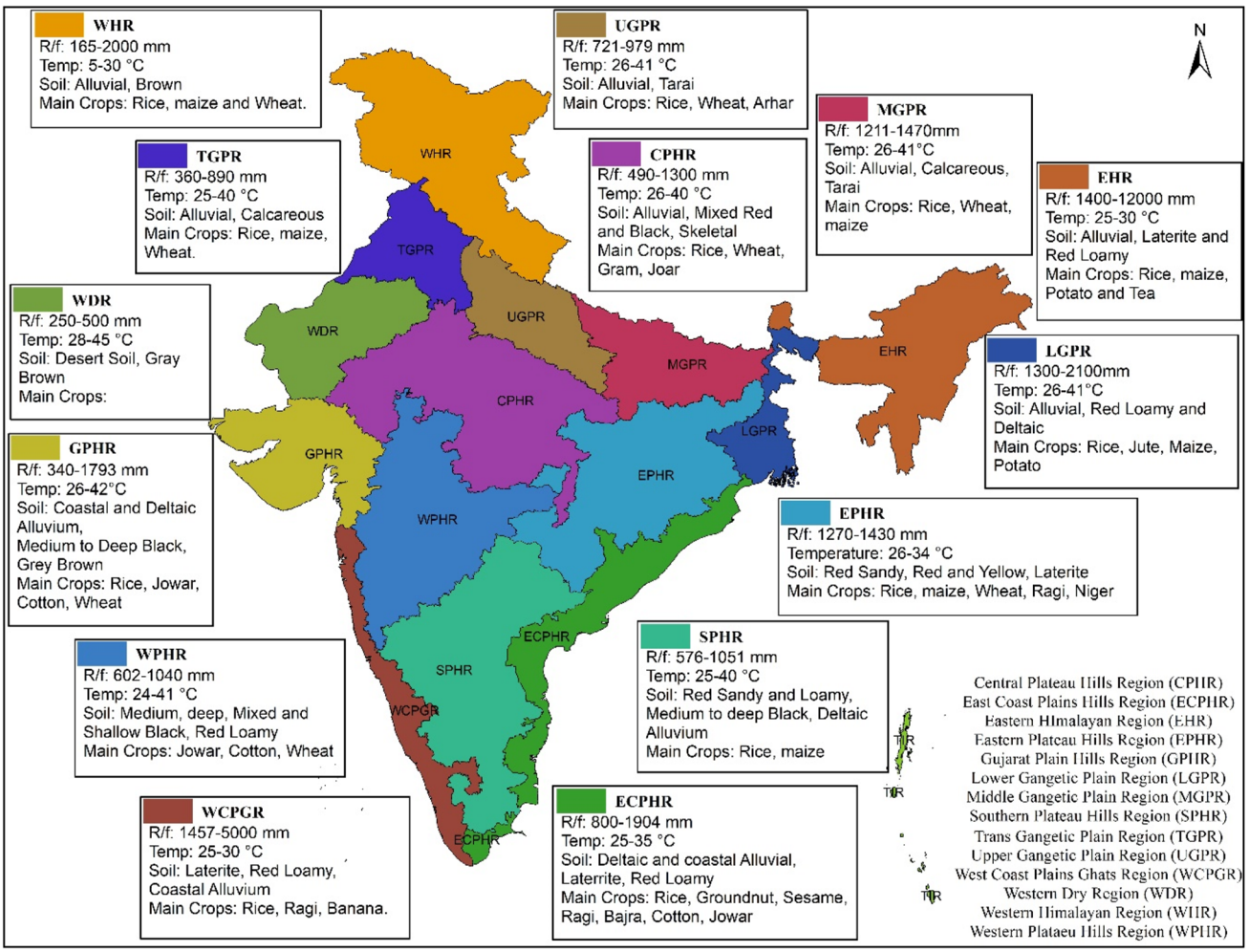

Fig. 1 Study site representing fourteen different agroclimatic zones of India

Giorgi et al. 2012) developed at The Abdus Salam International Centre for Theoretical Physics (ICTP), Italy, was obtained from the Mahamana Center of Excellence in Climate Change Research (DST-MCECCR), Banaras Hindu University (Singh et al. 2021d). The simulations were obtained at the same grid size (0.50° × 0.50°). LMDZ and CCAM ensembled were obtained from the Coordinated Regional Climate Downscaling Experiment-South Asia (CORDEX-SA) portal, managed in collaboration with the Centre for Climate Change Research (CCCR), and Indian Institute of Tropical Meteorology (IITM). The observed climate data over 1970–2005 are extracted from the India Meteorological Department (IMD) gridded data set (0.50° × 0.50°) for 1154 grids. We focus on the annual and seasonal analysis. Models are evaluated by comparing their historical simulations with observations over the period 1970–2005. Future changes are assessed by calculating differences between the historical period (1970–2005) and the future (2041–2060 and 2071–2099), in two distinct scenarios, namely, RCP4.5 and RCP8.5.

The fractional LULC comprising cropland (gcrop; a fraction of each grid cell in cropland), primary land (gothr; a fraction of each grid cell in primary land), secondary land (gsecd; a fraction of each grid cell in secondary land), and urban land (gurbn; a fraction of each grid cell in urban land) at 0.50° × 0.50° spatial resolution for the year 2005 based on HYDE 3.1 and future projections for the year 2050 and 2090 was obtained from four integrated assessment models (IAMs) and was used for the investigation of physical processes underlying DTR changes. These datasets are described in detail elsewhere (Hurtt et al. 2006, 2011).

All regionally averaged statistics are computed over the India region defined as the land grid points. Ultimately, all models have been taken with equal weights and considered in the present analysis for computing ensemble statistics.

2.3 Methodology

2.3.1 Bias correction

The outputs from the RCMs are generally biased and are rarely used directly. Therefore, it becomes imperative to correct the RCM outputs so that it adequately represents the actual climatic patterns. For this work, we used variance scaling (VS) to correct the biases in the RCM outputs. The details of this correction have been discussed in Bhatla et al. (2020). The statistical scores like percent bias (P_{bias}) and mean absolute error (MAE) were used to show relative bias and error estimation (P_{bias}, MAE) in the different RCMs computed against the IMD datasets for the baseline period 1981–2005 as follows: ACCESS (−1.08, 1.49), CCSM (−2.612, 1.66), CNRM (1.083, 1.68), GFDL (1.89, 1.63), MPI (1.76, 1.71). The values indicate comparatively less bias in the corrected RCM datasets and thus were used in the present analysis.

2.3.2 Trend analysis

In the present study, we used the modified Mann–Kendall test (MMK-test) proposed by Hamed and Rao (1998), to determine the long-term annual and seasonal trends in the temperature (Tmax, Tmin, and DTR) over past and projected climates for both the RCPs which accounts for the autocorrelation in the time series and thus, Kendall's tau and Sen's slope value are free of autocorrelation and data normalization. Kendall's tau and Sen's slope were used to detect the direction and amplitude of change in trend. The trend values at p (significance level) < 0.05 were considered significant.

2.3.3 Spatio-temporal change in DTR, Tmax, and Tmin in future

The change in DTR, Tmax, and Tmin in degree Celsius for each agroclimatic zones at annual and seasonal scales in the future period (2041–2060 and 2071–2099) for two RCPs is calculated by computing the relative change in temperature from the historical period (baseline; 1970–2005) using the formula:

$$\Delta T = T_F - T_H$$

where ΔT refers to the change in DTR, Tmax, and Tmin; T_F refers to the temperature in future; and T_H refers to the temperature in the historical period.

2.3.4 Change in LULC in future

The percentage change in fractional LULC in terms of gcrop, gothr, gsecd, and gurbn for each agroclimatic zone for the year 2050 and 2090 for two RCPs is calculated relative to the year 2005 using the following formula:

$$\Delta F_{LULC} = F_{HLULC} - F_{FLULC}$$

where ΔF_{LULC} refers to the percent change in the fraction of LULC in future; F_{HLULC} refers to fractional LULC in the historical year 2005; and F_{FLULC} refers to the fractional LULC in the future year 2050 and 2090.

2.3.5 Kernel density estimation (KDE)

Kernel density estimation (KDE) is a non-parametric approach to estimating the probability density function. The details of this can be found somewhere else (Wahiduzzaman and Yeasmin 2020). In this study, KDE is applied to evaluate the performance of different RCMs by comparing the distribution of DTR in different RCMs against the observed DTR. The KDE also shows the relative change in DTR in future in comparison to the past DTR.

3 Results and discussion

3.1 Kernel density estimation (KDE) analysis of DTR for different time periods and scenarios

KDEs of daily mean DTR for six model experiments for annual and seasons averaged over India are represented in Fig. 2. The figure provides an estimation of the temporal changes in DTR from historical climate to future as well as uncertainty in the model output. From the figure, it is very apparent that the model simulation underestimates the DTR by 0.08 °C compared to the observed annual basis which is contributed by underestimation in Tmax (0.46 °C) and Tmin (0.37 °C). Seasonal analysis shows that model simulations show agreement with the observed in winter and post-monsoon for DTR and Tmax and winter and pre-monsoon for Tmin, whereas high underestimation was observed in pre-monsoon for DTR and Tmax and in post-monsoon for Tmin. The model response to the increasing greenhouse gasses forcing with time is reflected as the decrease in the projected DTR under both scenarios for each time period. The simulated models show a decrease in DTR ranging from 0.27 to 0.31 °C in the RCP4.5 scenario to 0.35 to 0.71 °C in the RCP8.5 scenario annually. In seasons, the decrease in DTR ranges from 0.07 °C (post-monsoon) to 0.54 °C (pre-monsoon) in RCP4.5 and 0.07 °C (post-monsoon) to 1.10 °C (pre-monsoon) in RCP8.5 respectively in future compared to the historical period. CNRM and MPISM show a comparatively higher decline in DTR in future under RCP4.5, whereas NorESM

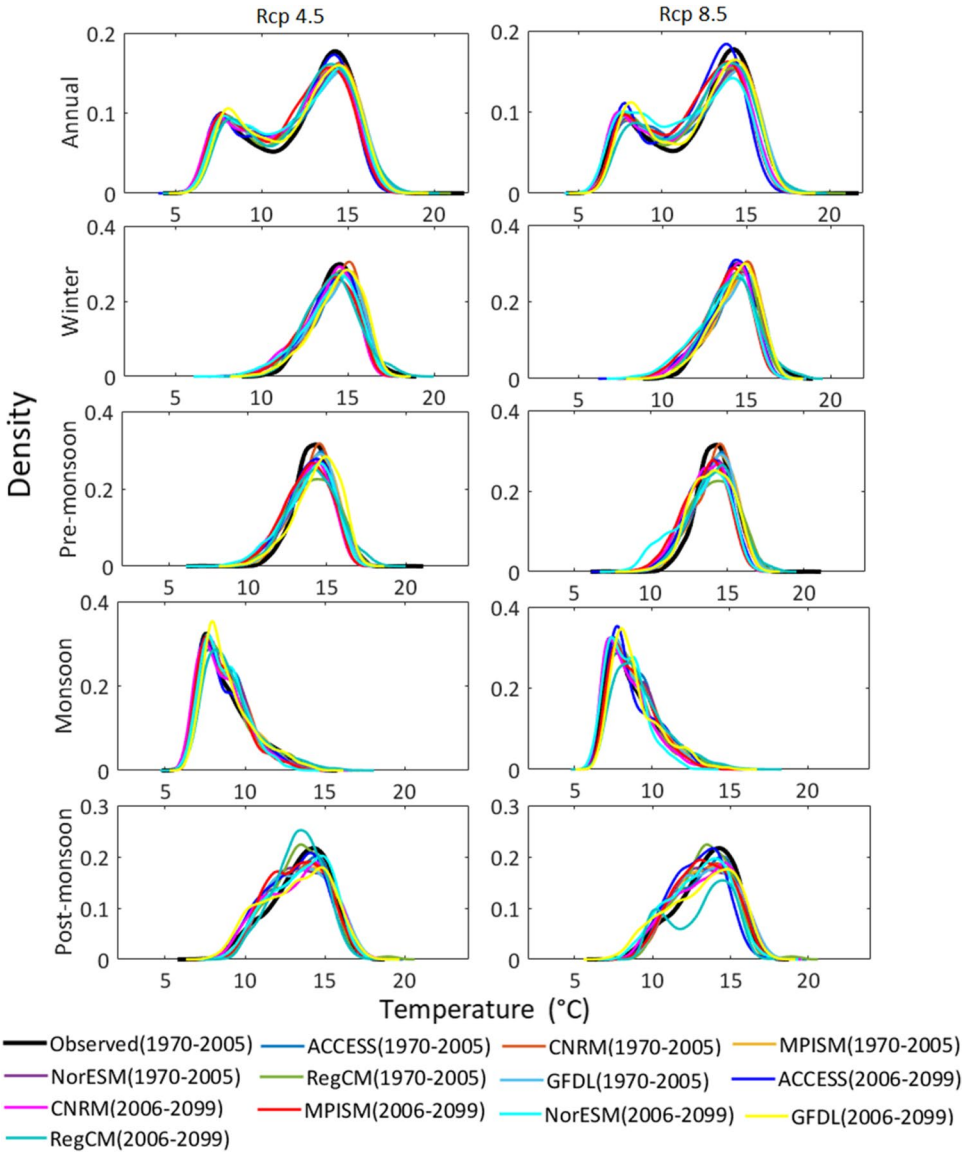

Fig. 2 KDE of annual and seasonal DTR (°C) for observed (1970–2005), historical (1970–2005), and future periods: mid-century (2041–2060) and far-century (2071–2099) for the two RCP scenarios RCP4.5 and RCP8.5 for different model experiments (RCMs)

shows a higher decline in DTR in RCP8.5. GFDL and RegCM4 show disagreement with the observed and with other models and mostly showed a rise in DTR in the future under both scenarios. Annually, most of the models show good distribution fit with the observed, but in seasons mainly in winter (both RCPs), pre-monsoon (mainly NorESM), and post-monsoon (RCP8.5) do not complement the observed data. A similar study by Zhuang and Zhang (2020), using a multimodel ensemble to analyze diurnal asymmetry in future, reported that the Indian subcontinent could witness a decrease in DTR up to 0 to 0.2 °C during 2020–2039 (RCP4.5) and up to 0.4 to 0.6 °C during 2080–2099 (RCP8.5) which is mainly attributed to increasing Tmin than Tmax.

3.2 Interannual and seasonal variability and trend of DTR, Tmax, and Tmin

The interannual and seasonal variability and trend of area-averaged DTR, Tmax, and Tmin is represented in Fig. 3, S1, and S2 and Table S1. Figure 3 helps to assess the uncertainty in the model projections, as well as how well the model could capture the variability in the observed data for the historical period (1970–2005). The variability is fairly consistent seasonally and annually for different model projections except for winter which shows high variability. Different model projections seemed to follow declining trends in DTR except for RegCM4 and NorESM. RegCM4 has shown a consistently increasing trend in DTR while NorESM had

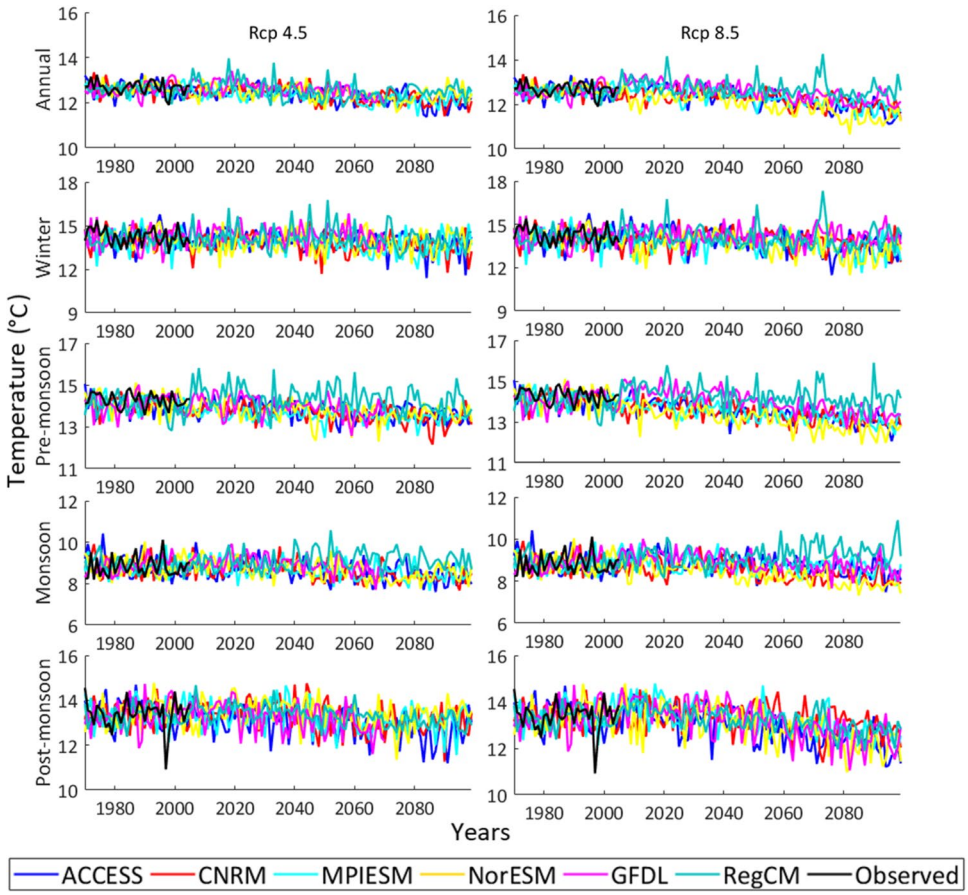

Fig. 3 Annual and seasonal variation of the DTR (°C) for the entire period of 1970–2099 for different model experiments (RCMs)

shown a consistent declining trend pretty much below the mean DTR shown by other models. GFDL on the other hand shows very high variability in the winter season (Fig. 3). Tmax and Tmin show a fairly consistent positive trend with different model projections, except GFDL which shows a relatively higher trend and RegCM4 which does not show a consistent trend relative to other models (Fig. S1 and Fig. S2).

The MMK trend test shows a decreasing trend of observed mean annual DTR (1970–2005) (0.001 °C/year) owing to a significant and higher increase in Tmin (0.013 °C/year) than Tmax (0.008 °C/year) (Table S1). The observations were supported by the model simulations of ACCESS, CNRM, NorESM, and RegCM4 which show a similar decline in DTR (0.001 to 0.012 °C/year). The decline in model DTR was complimented by the significant increase in Tmax (0.008–0.029 °C/year) and Tmin (0.018 to 0.026 °C/year) annually. Seasonal analysis for the observed period reveals neither DTR nor Tmax or Tmin (except in monsoon where Tmin showed a significant increase) showed any significant trend. On the other hand, the model simulation shows a significant decline in DTR in monsoon and post-monsoon by ACCESS and RegCM4 and in pre-monsoon by CNRM. Tmax and Tmin both show a significant increase in all four seasons, with a strong increase in Tmin during winter and pre-monsoon and Tmax during winter and post-monsoon.

In future, the mean annual DTR shows a decline (0.001 to 0.020 °C/year) and the rate of decline from mid-century to far-century or transition from scenario 4.5 to 8.5 was not necessarily high and mostly insignificant (Table S1, Fig. 3). The decline in DTR in RCP8.5 is supported by the higher (significant) increase in Tmin (max increase of 0.071 °C/year; GFDL) than Tmax (max increase of 0.060 °C/year; GFDL) (Table S1). Among different models, only MPIESM shows a significant decline under the far century period in RCP8.5. Moreover, models like MPIESM, NorESM, and RegCM4 reported inconsistencies in direction of change in DTR. However, a unidirectional decline in DTR was reported within seasons mostly (significant) in the RCP8.5 scenario, with the highest decline in DTR ranging from 0.038 °C/year (pre-monsoon, GFDL) in mid-century future of RCP4.5 to 0.039 °C/year (post-monsoon, ACCESS) in mid-century future of RCP8.5 (Table S1). Similarly, the seasonal

analysis showed a significant increase noted for Tmax and Tmin mostly in the RCP8.5 scenario by most of the models, with the maximum rate of warming for Tmax (0.092 °C/year; GFDL) and Tmin (0.091 °C/year; ACCESS and GFDL) reported in winter and post-monsoon respectively, but the rate of increase, in general, was higher for Tmin. The uncertainty in the model projections was also apparent, in which almost all the models showed a negative trend in Tmax and Tmin in annual and in different seasons but were limited to the RCP4.5 scenario and the increase was found to stabilize only in the RCP8.5 scenario (Fig. S1 and S2).

Though there lies a paucity of evidence on future changes in DTR as most of the literature focus on changes in Tmax and Tmin, yet most of the studies ascertain a high rise in Tmin than Tmax that eventually will be the reason behind declining DTR apart from other factors. Recent evidence of changes in DTR in the last several decades over India (Mall et al. 2021) emphasized a significant declining trend in DTR (− 0.02 °C/decade) post-1991 owing to a relative increase in Tmin (0.21 °C/decade, significant) compared to Tmax (0.18 °C/decade) with post-monsoon and monsoon months syncing with the trend. Similarly, Vinnarasi et al. (2017) found a decrease in DTR over different parts of India during 1981–2010, predominantly due to an increase in Tmin. The reason why DTR did not show any significant decline in the baseline period 1970–2005 in the present study is probably, the evident decline in both Tmax and Tmin occurred only after 1991, and thus the overall trend was insignificant. The findings of the present study are consistent with the study of Sharma and Goyal (2020) who reported that Tmax shows high uncertainty under future scenarios and the increasing trend stabilized in RCP4.5, but a consistently increasing trend was noticed for RCP8.5. Tmin on the other hand shows less uncertainty. Zhuang and Zhang (2020), using a multimodel ensemble to analyze diurnal asymmetry in future, reported that the Indian subcontinent could witness a decrease in DTR up to 0 to 0.2 °C during 2020–2039 (RCP4.5) and up to 0.4 to 0.6 °C in 2080–2099 (RCP8.5) mainly attributed to increase in Tmin. Kundu et al. (2017) used HADCM3 data (A2 scenario) to report a high rise of Tmin in winter and Tmax in the pre-monsoon with the end century period predicted to show the highest increment (2081–2099) in central India. Dash et al. (2012) indicated a rise in the annual mean temperature (Tmean) using simulations from RegCM3 between 0.64 °C (2011–2040) and 5 °C (2071–2100) relative to 1981–2010. Kumar et al. (2021) used 21 CMIP5 GCMs simulations over 24 major river basins of India for the period 1950–2005 and 2006–2100 under RCP4.5 and RCP8.5 to show an increase in Tmax (pre-monsoon) and Tmin (winter) with the overall increasing trend of 0 to 0.50 °C/decade under RCP4.5 and mostly, above 0.50 °C/decade under RCP8.5.

3.3 Spatial trend

3.3.1 The annual variation

Figures 4, 5, and S3-S6 display the spatial distributions for the changes in zonal averages of DTR, Tmax, and Tmin for the future period: 2041–2060 and 2071–2099 relative to the historical period 1970–2005 at annual and seasonal levels under RCP4.5 and RCP8.5 scenario. The entire upper half of India including the northern (most parts of WHR, TGPR, UGPR), central (CPHR and parts of WPHR), north western (WDR and GPHR), and eastern part of India (MGPR, LGPR, EPHR) showed a declining DTR during the mid-century and far-century future under RCP4.5 ranging from 0.25 to 3 °C in simulations from ACCESS, CNRM, MPISM, and NorESM whereas the plateau region (WPHR, SPHR, and EPHR), coastal region (ECPHR and WCPGR), and Northeast Himalayas (EHR) show an increase in DTR varying from 0.5 to 1 °C. The spatial trend, however, also showed model uncertainties within the different RCM simulations used. Among the six RCMs used, simulations by RegCM4 did not act in accordance with the same changing pattern in DTR as other models; instead, it showed a unanimous increase in DTR over most parts of India (0.5 to 2 °C) irrespective of the time period and scenario.

In the RCP8.5 that is characterized by a significant increase in GHG concentration, a similar pattern of changes was observed in the early century period as in RCP4.5; however, there is a remarkable decline in DTR evident over most of the regions in the far century period except in WHR and EHR in most of the model simulations except RegCM4 (change in DTR by − 0.5 to + 1 in both the time periods; RCP8.5). However, the large decline in DTR was still limited to the northern and central parts (0.75 to 3 °C) (Fig S4) attributed to the higher increase in Tmin. As visible in Fig S3 and S4, in the RCP4.5 scenario, mid-century period, the increase in Tmax over the northern, central, and western regions of India varied from 1 to 1.5 °C, whereas the increase in Tmin ranged from 1.5 to 2 °C. In the far century period, the difference between the Tmax (0.5 to 2 °C) and Tmin (1.25 to 3 °C) increased further. The same trajectory was followed in the RCP8.5 with the difference between the rise in Tmin to Tmax being 1.5 °C in the mid-century to 3.5 °C in the far century period (Fig. S5 and S6). The Similar piece of evidence came from Praveen et al. (2016) who shows an overall decreasing trend in DTR in future over the southern India under RCP8.5. Zhuang and Zhang (2020) also reported declining DTR over the Indian region (0 to 0.2 °C) in both time periods and scenarios with a higher decline in the far century period of RCP8.5 (0.6 to 0.8 °C); however, the magnitude of decline was less compared to the present study.

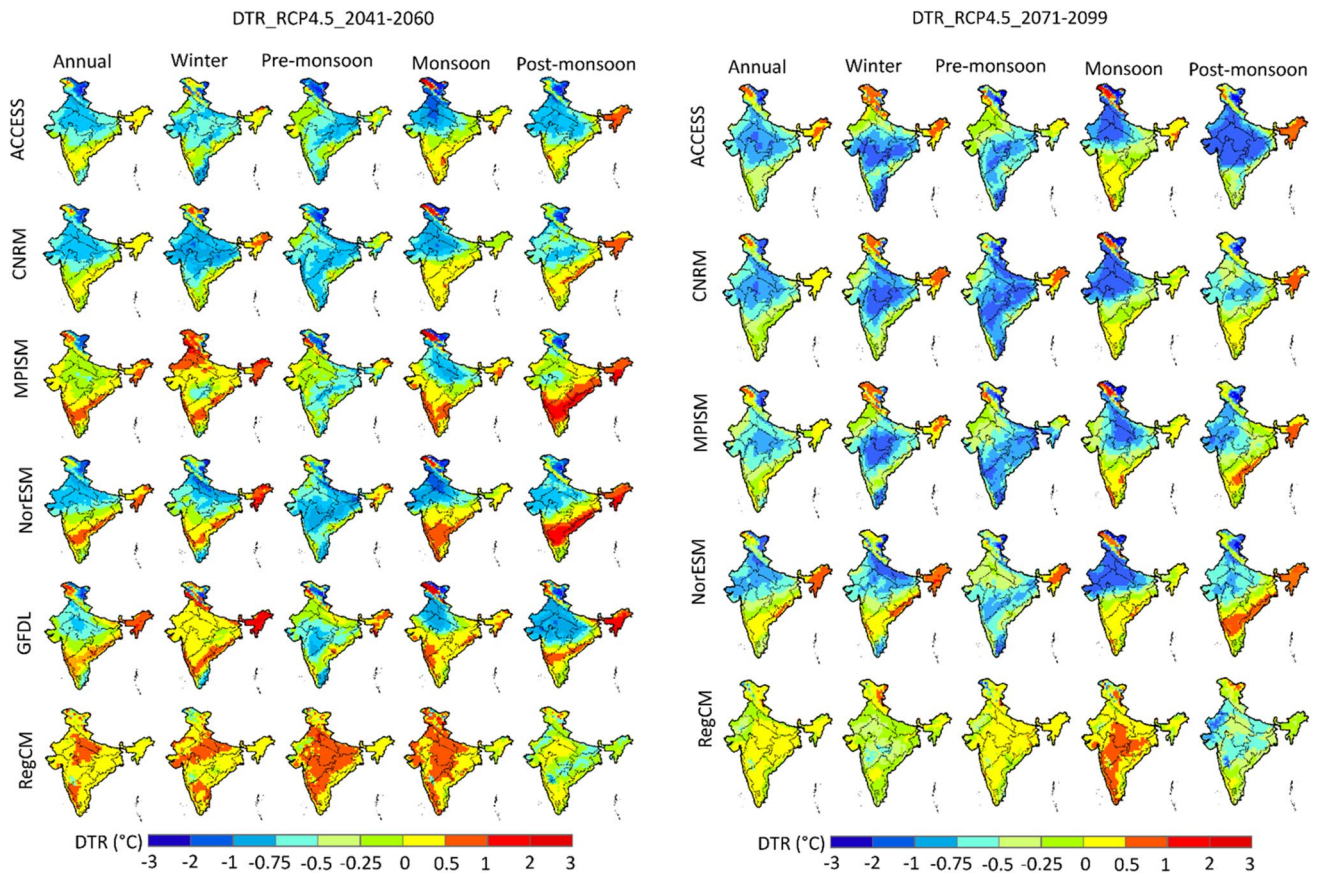

Fig. 4 Change in annual and seasonal the DTR (°C) under RCP4.5 mid-century (2041–2060) and far-century (2071–2099) period for different model experiments (RCMs)

3.3.2 The seasonal variation

The seasonal analysis of DTR did not show any prominent distinguishable change in DTR in any particular season. Large model uncertainty was found during the winter season in mid-century under both scenarios in which MPISM, GFDL, and RegCM4 show an overall increase in DTR in RCP4.5 prominently over part of the Himalayan region (WHR, EHR) and southern plateau region (ECPHR, SPHR, and WCPGR) while ACCESS, CNRM, and NorESM show a decline in central (CPHR, WPHR), northern (TGPR, UGPR, MGPR), eastern (LGPR and EPHR), and western (WDR and GPHR) India (Fig. 4). However, during 8.5, the decline in DTR was low than RCP4.5 except in NorESM and MPISM. In the far century future, the overall decrease in DTR was high, particularly in RCP8.5 (Fig. 5). The prominent region of decline is mainly concentrated over central India in the far century period in both the scenarios up to 3 °C extending to the south shown by most of the models except GFDL and RegCM4. Pre-monsoon season shows a decline in DTR in most of the agroclimatic zones, which is slightly skewed towards central, eastern, and southern India and prominent during the end of the century varying from 0.5 to 3 °C in both scenarios. Most of the models showed a similar pattern of change with some differences in terms of spatial coverage and the absolute value of decline in DTR, except GFDL (0 to 2 °C, mid-century, RCP4.5) and RegCM4 (0 to 2 °C, with large variations) which mostly showed an increase in DTR. During monsoon, the decline is mainly limited to the north, central, and western regions in both periods and scenarios ranging from 0.5 to 3 °C, with RCP8.5 far century period showing the highest decline. MPISM and GFDL show a different pattern of spatial decline in comparison to other models, and RegCM4 shows an overall increase (0 to 1 °C in all scenarios and 0 to 3 °C in RCP8.5, far century future) in most of the agroclimatic regions. Likewise, in other seasons, the decline in DTR in the post-monsoon season is mainly limited to the upper half region of India (0.75 to 2 °C) and the increase is mostly noted in part of southern India covering plateau and coastal regions. The decline in DTR was unanimous in simulations from all the models but the spatial extent and magnitude of decline were large in RCP8.5 far century

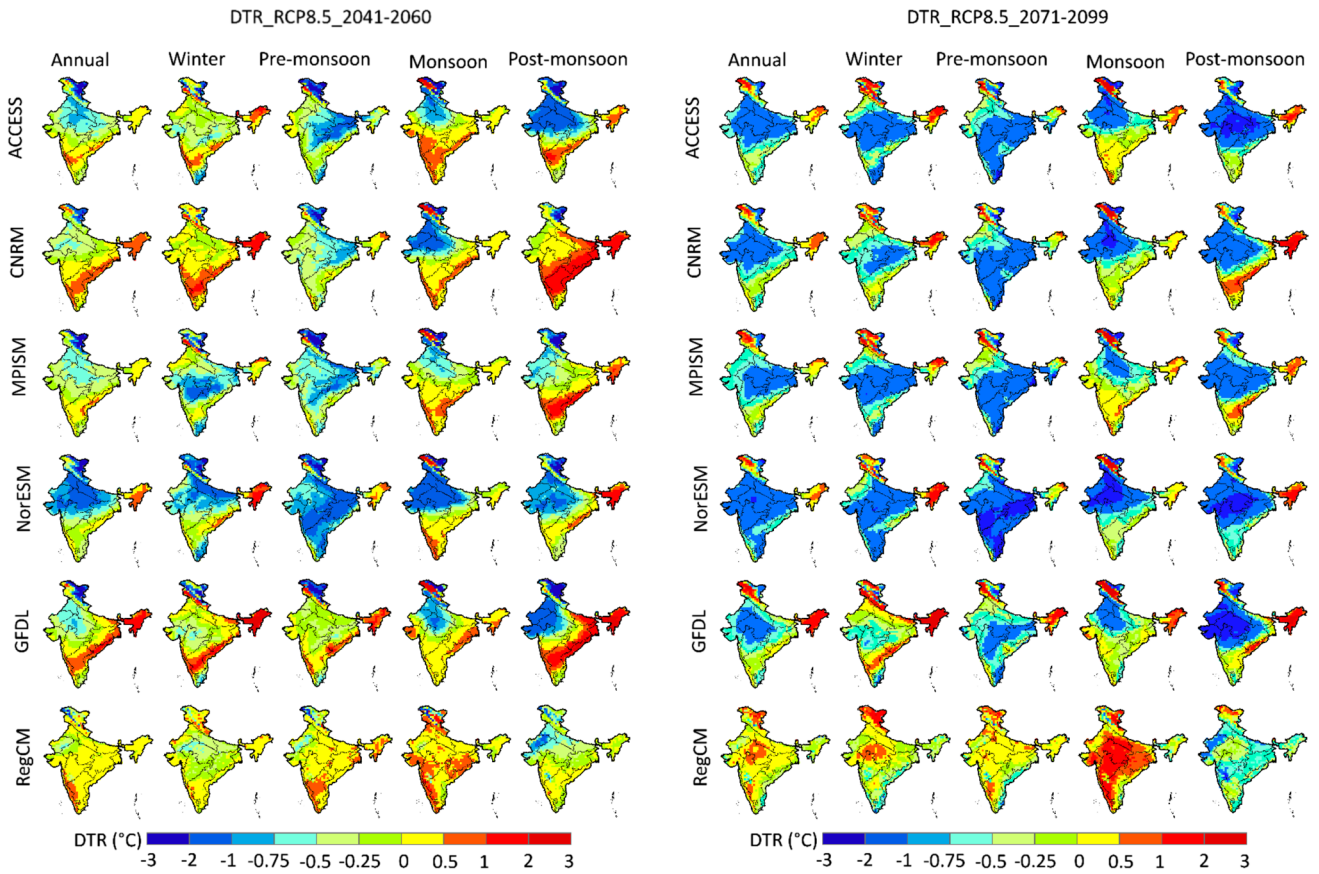

Fig. 5 Change in annual and seasonal DTR (°C) under RCP8.5 mid-century (2041–2060) and far-century (2071–2099) period for different model experiments (RCMs)

future (by 3 °C). However, CNRM and RegCM4 showed deviations from other models in midcentury RCP4.5 and RCP8.5, respectively.

The seasonal analysis of Tmax and Tmin shows remarkable warming during winter and cooling in monsoon in comparison to other seasons as shown by simulations from ACCESS, MPISM, and GFDL, with an increase in temperature ranging from 2 to 4 °C in RCP4.5 and up to 6 °C in RCP8.5 scenario (Fig S3-S6). Moreover, ACCESS and GFDL in most of the seasons show intense warming over various agroclimatic regions in comparison to other models. Other models too showed an increase in Tmax (0.5 to 2.5 °C) and Tmin (1.5 to 4.5 °C) with Tmin showing a relatively higher rate of increase. The rise in Tmax and Tmin in pre-monsoon season is mostly concentrated over northern agroclimatic zones TGPR, UGPR, CPHR, WDR, and parts of plateau region (WPHR, and GPHR), in all the model simulations except RegCM4. The rise in Tmax in pre-monsoon ranged from 1 to 2.5 °C in RCP4.5 to 1 to 4 °C in RCP8.5 and Tmin from 1.5 to 2.5 °C in the mid-century future of RCP4.5 scenario to 3.5 to 6 in RCP8.5 (Fig. S3-S6). Interestingly, agroclimatic zones covering coastal, plateau, and lower Gangetic regions show a decline in Tmax or a very sparse increase while the rise in Tmin was comparatively much greater which caused a prominent decline in DTR in these regions. During monsoon season, the increase in Tmax was apparent in parts of the plateau region (WPHR, SPHR, and EPHR), coastal region (ECPHR and WCPGR), and Northeast India (EHR) in both periods and scenarios up to 1 to 2 °C while most of northern India shows a very slight increase to decline in Tmax (− 1 to 1 °C) in all model simulations except GFDL and RegCM4. The decline was spatially more consistent in the far century period in both scenarios. The increase in Tmin on the other hand ranged from 1 to 1.5 °C in RCP4.5 and 2 to 3.5 °C in RCP8.5. The high rise in Tmin in parts of northern and western India caused a decline in DTR whereas relative increase in Tmax in some parts of the east coast and west coast and SPHR caused a rise in DTR. In other parts, the DTR showed unnoticeable change. During post-monsoon season, the increase in the Tmax was higher over the plateau, coastal, and Himalayan region (1.5 to 3 °C) and less over the northern agroclimatic region (1 to 2.5 °C) in RCP4.5. In the far century period,

the model simulations do not show any consistent pattern altogether but showed an increase mostly ranging from 0.5 to 3 °C (Fig S3-S6). Tmin, on the other hand, showed an increase of 1.5 to 2 °C in the mid-century and 1.5 to 2.5 °C in the far-century period. GFDL and ACCESS showed model uncertainty and reported a large increase in mid-century and far-century, respectively. This large increase was mostly concentrated in the northern and central parts while other regions showed an increase varying from 0.5 to 1.5 °C. In the 8.5 scenarios, the Tmax show little consistent warming in the range of 2 to 2.5 °C in the upper half region of India and 2 to 4 °C in the lower part, whereas, in the far century future, the warming inconsistently varied from 1 to 2.5 °C covering most of the agroclimatic zones. On the other hand, Tmin showed an increase of 3 to 4.5 °C mostly concentrated in the northern part. A higher Tmin than Tmax caused a decline in DTR in the northern and central parts that further intensified spatially in the RCP8.5 scenario, whereas a rise in Tmax greater than Tmin led to a rise in DTR in the southern and north eastern part.

The results of this study are consistent with the findings of previous studies. The multimodel ensemble (MME) mean projections over the world show warming in both the time periods (2020, 2039) and scenarios (RCP4.5 and 8.5), with higher warming, was reported in RCP8.5 far century period. The warming was higher in the WHR and Gangetic plain region, with Tmin slightly higher than Tmax in the far century period. The DTR showed a slight decrease in all two scenarios and periods with a higher decrease in WDR (Zhuang and Zhang 2020). A similar piece of evidence is reported in the study over the Teesta River basin in Eastern Himalayas (EHR) that used four different GCMs and two RCP scenarios (RCP4.5 and RCP8.5) that show an increase in the Tmax and Tmin both but a high increase in Tmax that leads to increase in DTR in the region in the RCP4.5 scenario. The Tmin climatology shows a higher rate of increase over high altitude regions by Dimri et al. (2018). Similar evidence of warming particularly during winter time is also reported over the Koshi river basin using CMIP5 GCM analysis (Rajbhandari et al. 2016); over the Indus river basin using PRECIS (Rajbhandari et al. 2015); over the Hindukush-Himalaya-Karakoram region (Wiltshire 2014) and Hindukush Himalayas (Sanjay et al. 2017). However, in these studies, the increase in Tmax and Tmin shows the same rate of increase in the 8.5 scenarios, thus no substantial change in DTR was observed, unlike our study shows an increase in DTR over EHR in both scenarios (Sharma and Goyal 2020). Dash et al. (2012) further reported an increase in the annual mean surface temperature by about 0.64 °C in the coming 30 years from 2011 to 2040 and by 5.15 °C at the end of the century (2071–2100).

3.4 Fractional change in LULC in future

In this study, the change in the fraction of four important land use states has been calculated to better understand the physical reasons for the changes in Tmax, Tmin, and DTR in future. Figure 6 shows that spatially aggregated magnitudes of key land use states are generally quite similar for the mid (2050) and far-century periods (2090) except for gcrop. A remarkable increase in gcrop fraction was observed up to 50% and in some grids up to 97% in parts of EHR, WHR, UGPR, MGPR, LGPR, and WCPGR in 2090 with a slight decline of 7% in most parts of 2050 in RCP4.5. In the 8.5 scenarios, gcrop mostly showed mix pattern with a prominent increase limited to the northern part (up to 20%). An overall increase in the fraction was noted for gothr in both scenarios, but a decline was evident from RCP4.5 to 8.5 in TGPR, WDR, GPHR, and parts of CPHR and WPHR up to 40% (Fig. 6). In past too there have been instances in which some parts of India were able to achieve a land use transition in a manner such that there was an increase in agricultural production and forest cover simultaneously (Lambin and Meyfroidt 2011). Importantly, gsecd on the other hand mostly showed a decrease varying from 0 to 40%, with some grids in HER, WDR, CPHR, WPHR, and EPHR showing a decline up to 40 to 55% and the decline further increased to 25 to 75% in RCP8.5 in comparison to 2005. However, the entire northern states covering agroclimatic zones WHR, EHR, TGPR, UGPR, MGPR, LGPR, and WCPGR shows an increase varying from 0 to 2% in RCP4.5 and up to 32% in RCP8.5. The fraction of urban land did not change much in the RCP4.5 scenario when compared to 2005 with very few grids in the Gangetic plain showing a slight decline. In the 8.5 scenarios, the urban land decline is prominent in parts of the TGPR, LGPR, and southern part of SPHR, WCPGR, and ECPHR.

The increased fraction of gcrop, decreasing gothr from RCP4.5 to 8.5 and decreasing gsecd in regions of northern, central, and western India, could roughly explain the reason for a unanimous decline in DTR in most of the agroclimatic regions in the northern part and an increase in DTR in the eastern and southern plateau region and coastal regions. The additional agricultural land use could reduce carbon storage and reduce forest habitat for biodiversity and have other negative impacts on ecosystem services (Sala et al. 2000), which is partially offset by an increase in primary land (Pereira et al. 2010; Hurtt et al. 2011). In general, the LULC significantly controls the DTR change through the changes in canopy evaporation and transpiration (Hua et al. 2013). The land-use changes may bring changes in the surface albedo, surface aerodynamic roughness, and terrestrial carbon balance, with further repercussions on regional-global atmospheric general circulation, weather, hydrology, and climate (Pielke et al. 2002; Piao et al. 2007;

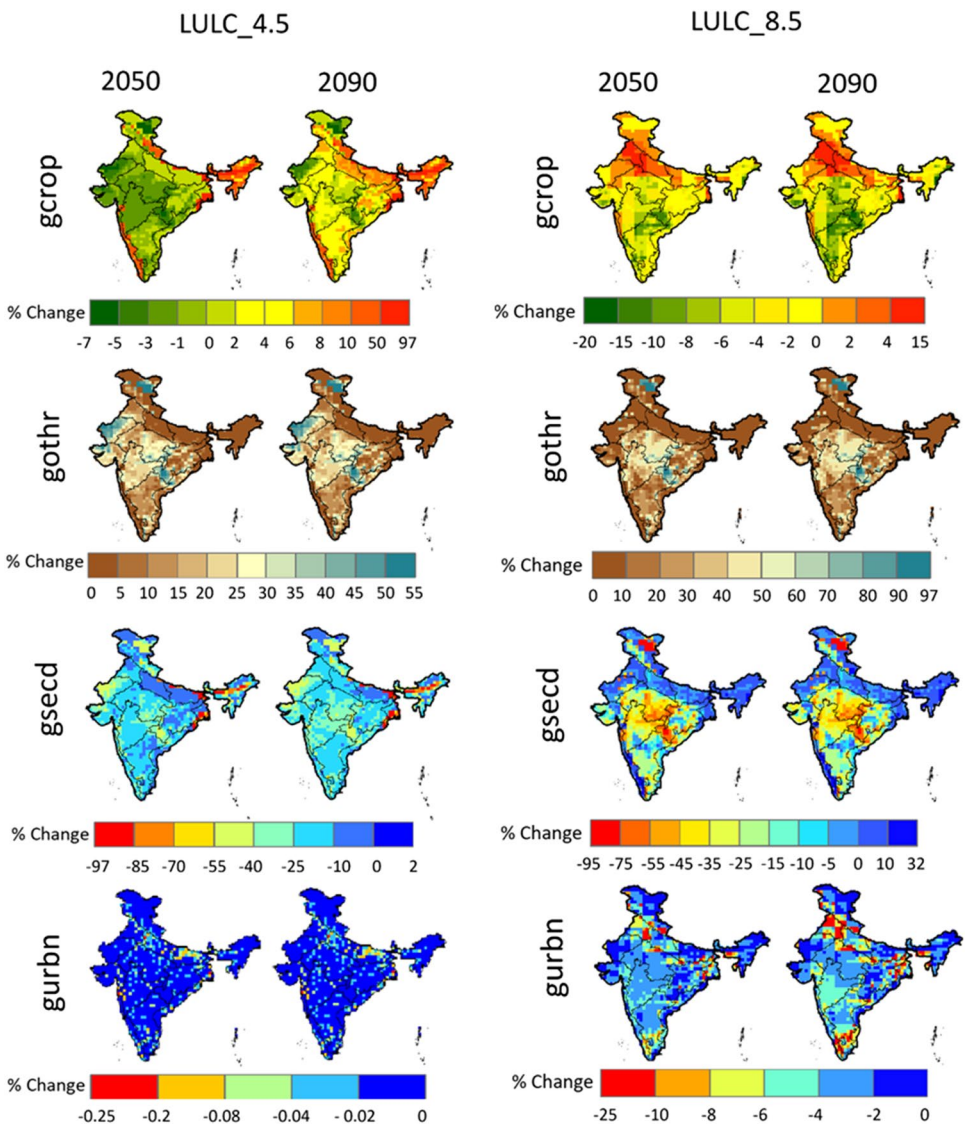

Fig. 6 Percentage (%) fractional change in each grid cell under RCP4.5 and RCP8.5 for gcrop (cropland), gothr (primary land), gsecd (secondary land), and gurbn (urban land) over the different agroclimatic zones of India for the year 2050 and 2090

Pitman et al. 2009; Shevliakova et al. 2009; Pongratz et al. 2010; Hurtt et al. 2011). In a separate study, different RCPs project large increases in wood harvest and resulting secondary lands up to 35–75% and between 6.0 and 13.27% across the years 2015 to 2100, and most of the increase is suspected on potentially forested land causing reductions in primary land by 2100 (Hurtt et al. 2011, 2020). However, the parts in northern agroclimatic zones that show a rise in cropland and a decline in secondary land clearly indicate the rising human disturbances by either the conversion of secondary land to cropland or being utilized for other anthropogenic activities. Thus, while secondary land may actually increase under some scenarios, remaining secondary land may be more impacted overall. Thus, secondary land might play an important role in Earth system dynamics in the future. The approach to providing annual global gridded land-use transitions data from past to future relies on a combination of multiple model inputs and other model factors that could be considered uncertain and would need consistent improvements. Further, urbanization can produce remarkable impacts on DTR (Kalnay and Cai 2003; Zhou et al. 2004; Hua et al. 2013).

Apart from LULC the Gangetic plain that showed a consistent decrease in DTR in the present and future is often a center of investigation due to the persistence thick aerosol layer over it (IGP; Kumar et al. 2018) which was reported to exceed aerosol optical depth (AOD) > 0.8 during post-monsoon (Singh et al. 2018) and winter seasons (Kumar et al. 2018). The high AOD over IGP has been indirectly linked to high cloud cover and solar dimming causing a rise in Tmin (Hu et al. 2017; Soni et al. 2012). Srad displayed a gradual increase varying from 0.013 to 0.027 MJ m^{-2} day^{-1} in different regions of India but the northern Himalayan region (0.047 MJ m^{-2} day^{-1}) and Gangetic plain region

(0.028 MJ m^{-2} day^{-1}) showed a declining trend. Even the increase in Srad was not consistent as it decreased significantly over different regions consistently from 2006 (0.447 to 0.090 MJ m^{-2} day^{-1}). Further, recent evidence shows 0.5–4% radiation dimming by 2030–2059 with uncertainties as high as 10% (relative to 1971–2000), in sync with rising aerosol and water vapor dimming (Ruosteenoja et al. 2019) with the largest reduction is anticipated for northern India. Nevertheless, further studies concerning the mechanisms of changes in DTR are still needed.

The study has its strengths and limitations. The study presents impressive information about the change in DTR, Tmax, and Tmin in the two different time periods in the future in two possible emission scenarios taking into consideration the uncertainties associated with different climate models at a finer regional scale of fourteen agroclimatic zones of India. The study employed RCMs over GCMs that can provide better regional information. The study also took into consideration the possible changes in LULC in the contemporary period that could strongly influence the DTR in a region. As India is characterized by a diverse climatic zone, any generalization without accounting for regional variances would be inadequate and inefficient. This issue has been recognized in the present study and quantified. However, the results are limited by several uncertainties. The first one is the uncertainty in the model projections at both the temporal and spatial scales. Like, RegCM4 and NorESM do not show good agreement with the other models in simulating mean DTR, whereas GFDL and RegCM4 do not show fairly consistent trends for Tmax and Tmin. The DTR is strongly affected by changes in incoming radiation, cloud cover, and aerosol loading, which was not analyzed in the present study that may influence the conclusion of the present study.

4 Conclusions

Our results indicate a decrease in DTR in the future climate but the rate of decline was not necessarily higher in high-emission scenarios. On contrary, Tmax and Tmin displayed a significant increase both in past and future, particularly in the high-emission scenario (RCP8.5), with Tmin showing a relatively higher increase than Tmax. The seasonal analysis reported no significant change in observed DTR, Tmax, and Tmin; however, for the same period, models did show a significant increase in Tmax and Tmin in all four seasons, with a strong increase in Tmin during winter and pre-monsoon and Tmax during winter and post-monsoon. Moreover, DTR displayed a significant decline in different seasons in future particularly in pre-monsoon and post-monsoon, while Tmax and Tmin reported a maximum decline in winter and post-monsoon, respectively.

The spatio-temporal analysis revealed that the upper half of India including the northern (most parts of WHR, TGPR, UGPR), central (CPHR and parts of WPHR), north western (WDR and GPHR), and eastern part of India (MGPR, LGPR, EPHR) showed a declining trend in DTR that is more prominent in high-emission scenario owing to a high rise in Tmin over Tmax. Contrarily, the plateau region (WPHR, SPHR, and EPHR), coastal region (ECPHR and WCPGR), and Northeast India (EHR) showed an increase in DTR. A large uncertainty exists about the change in DTR within the seasons such as the midcentury period of both RCPs shows a hotspot of declining DTR centered in northwestern and central India, while the hotspots shifted towards northeastern, central, and southern India in the far century future in winter and pre-monsoon.

The increasing gcrop, and decreasing gothr and gsecd from RCP4.5 to 8.5 in regions of central and western India, could roughly explain the reason for a unanimous decline in DTR in most of the agroclimatic regions in the northern part and the increase in DTR in the eastern and southern plateau region and coastal regions. This explains that increased LULC and land deterioration is an unsustainable practice and will possibly give rise to undesirable consequences such as climate change. The decline in DTR could interfere with the human circadian cycle, causing adverse health impacts, and could also interfere with the crop cycle, causing a loss in quality and quantity of crop yield. DTR could also influence the activity of nocturnal animals and thus might affect biodiversity as a whole.

The study attempts to provide evidence of change in DTR and other important factors at a regional scale in India using multimodel ensembling that can be utilized by stakeholders and policymakers to develop climate change adaptation strategies to deal with its possible implications on different sectors such as water resource management, agricultural, and health planning.

Supplementary Information The online version contains supplementary material available at https://doi.org/10.1007/s00704-023-04407-2.

Acknowledgements The authors gratefully acknowledge the World Climate Research Programme's Working Groups, the former coordinating body of CORDEX and CMIP5 for producing and making the data available. The authors thank the Earth System Grid Federation (ESGF) infrastructure and the Climate Data Portal hosted at the Centre for Climate Change Research (CCCR), Indian Institute of Tropical Meteorology (IITM), for providing CORDEX South Asia data. The authors also thank the India Meteorology Department (IMD) for providing the observed climate dataset. The authors also thank the Land-Use Harmonization 2 (LUH2) project for making their datasets freely available for use.

Author contribution Nidhi Singh: conceptualization, methodology, formal analysis, interpretation, review and writing of the original draft; Manisha Chaturvedi: methodology, formal analysis, interpretation; R K Mall: conceptualization, methodology, interpretation as well as review and editing of the draft, resources, funding acquisition, supervision, project administration.

Funding Authors thank the Climate Change Programme, Department of Science and Technology, New Delhi, for financial support (DST/CCP/CoE/80/2017(G)).

Data availability The CMIP5-CORDEX South Asia data available from Centre for Climate Change Research (CCCR), Indian Institute of Tropical Meteorology (IITM) at http://cccr.tropmet.res.in/home/esgf_node.jsp. Observed data available from the India Meteorology Department (IMD) at http://www.imdpune.gov.in/Clim_Pred_LRF_New/Grided_Data_Download.html. The Land-Use Harmonization 2 (LUH2) data were available at https://daac.ornl.gov/VEGETATION/guides/LUH2_GCB2019.html.

Code availability Authors declare that all software application and custom code support their published claims and comply with field standards.

Declarations

Conflict of interest The authors declare no competing interests.

References

Bhatla R, Sarkar D, Verma S, Sinha P, Ghosh S, Mall RK (2020) Regional climate model performance and application of bias corrections in simulating summer monsoon maximum temperature for agro-climatic zones in India. Theoret Appl Climatol 142(3):1595–1612

Bhatt D, Sonkar G, Mall RK (2019) Impact of climate variability on the rice yield in Uttar Pradesh: an agro-climatic zone-based study. Environ Process 6(1):135–153

Braganza K, Karoly DJ, Arblaster JM (2004) Diurnal temperature range as an index of global climate change during the twentieth century. Geophys Res Lett 31(13)

Cattiaux J, Douville H, Schoetter R, Parey S, Yiou P (2015) Projected increase in diurnal and interdiurnal variations of European summer temperatures. Geophys Res Lett 42(3):899–907

Cox DT, Maclean IM, Gardner AS, Gaston KJ (2020) Global variation in diurnal asymmetry in temperature, cloud cover, specific humidity and precipitation and its association with leaf area index. Glob Change Biol 26(12):7099–7111

Cubasch U, Wuebbles D, Chen D, Facchini MC, Frame D, Mahowald N, Winther J-G (2013) IPCC-AR5, IPCC: working group I contribution to the IPCC fifth assessment report climate change 2013: the physical science basis

Dai A, Trenberth KE (2004) The diurnal cycle and its depiction in the Community Climate System Model. J Clim 17(5):930–951

Dai A, Trenberth KE, Karl TR (1999) Effects of clouds, soil moisture, precipitation, and water vapor on diurnal temperature range. J Clim 12(8):2451–2473

Dash SK, Sharma N, Pattnayak KC, Gao XJ, Shi Y (2012) Temperature and precipitation changes in the north-east India and their future projections. Global Planet Change 98:31–44

Dey S, Di Girolamo L (2011). A decade of change in aerosol properties over the Indian subcontinent. Geophys Res Lett 38(14)

Dimri AP, Kumar D, Choudhary A, Maharana P (2018) Future changes over the Himalayas: maximum and minimum temperature. Global Planet Change 162:212–234

Dubey PK, Chaurasia R, Pandey KK, Bundela AK, Singh A, Singh GS, Mall RK, Abhilash PC (2023) Double transplantation as a climate resilient and sustainable resource management strategy for rice production in eastern Uttar Pradesh, north India. J Environ Manag 329:117082. https://doi.org/10.1016/j.jenvman.2022.117082

Fischer EM, Rajczak J, Schär C (2012) Changes in European summer temperature variability revisited. Geophys Res Lett 39(19)

Giorgi F, Coppola E, Solmon F, Mariotti L, Sylla MB, Bi X, ... Brankovic C (2012) RegCM4: model description and preliminary tests over multiple CORDEX domains. Clim Res 52:7–29

Hamed KH, Rao AR (1998) A modified Mann-Kendall trend test for autocorrelated data. J Hydrol 204(1–4):182–196

He B, Huang L, Wang Q (2015) Precipitation deficits increase high diurnal temperature range extremes. Sci Rep 5(1):1–7

Hu B, Zhao X, Liu H, Liu Z, Song T, Wang Y, ..., Xin J (2017) Quantification of the impact of aerosol on broadband solar radiation in North China. Sci Rep 7(1):1–8

Hua W, Chen HC (2013) Impacts of regional-scale land use/land cover change on diurnal temperature range. Adv Clim Change Res 4(3):166–172

Hurtt GC, Frolking S, Fearon MG, Moore B, Shevliakova E, Malyshev S, ..., Houghton RA (2006) The underpinnings of land-use history: three centuries of global gridded land-use transitions, wood-harvest activity, and resulting secondary lands. Glob Change Biol 12(7):1208–1229

Hurtt GC, Chini LP, Frolking S, Betts RA, Feddema J, Fischer G, ..., Wang YP (2011) Harmonization of land-use scenarios for the period 1500–2100: 600 years of global gridded annual land-use transitions, wood harvest, and resulting secondary lands. Clim Change 109(1):117–161

Hurtt GC, Chini L, Sahajpal R, Frolking S, Bodirsky BL, Calvin K, ..., Zhang X (2020) Harmonization of global land use change and management for the period 850–2100 (LUH2) for CMIP6. Geosci Model Dev 13(11):5425–5464

IPCC (2021): Climate change 2021: the physical science basis. Contribution of Working Group I to the Sixth Assessment Report of the Intergovernmental Panel on Climate Change [V Masson-Delmotte, P Zhai, A Pirani, SL Connors, C Péan, S Berger, N Caud, Y Chen, L Goldfarb, MI Gomis, M Huang K Leitzell, E Lonnoy, JBR Matthews, TK Maycock, T Waterfield, O Yelekçi, R Yu, and B Zhou (eds.) Cambridge University Press. In Press

Jaiswal R, Mall RK, Patel S, Singh N, Mendiratta N, Gupta A (2023) Indian sugarcane under warming climate: a simulation study. Eur J Agron 144:126760. https://doi.org/10.1016/j.eja.2023.126760

Kalnay E, Cai M (2003) Impact of urbanization and land-use change on climate. Nature 423(6939):528–531

Karl TR, Jones PD, Knight RW, Kukla G, Plummer N, Razuvayev V, ..., Peterson TC (1993) Asymmetric trends of daily maximum and minimum temperature. Papers Natural Resour 185

Karl TR, Kukla G, Razuvayev VN, Changery MJ, Quayle RG, Heim Jr RR, ..., Fu CB (1991) Global warming: evidence for asymmetric diurnal temperature change. Geophys Res Lett 18(12):2253–2256

Kumar M, Parmar KS, Kumar DB, Mhawish A, Broday DM, Mall RK, Banerjee T (2018) Long-term aerosol climatology over Indo-Gangetic Plain: trend, prediction and potential source fields. Atmos Environ 180:37–50

Kumar N, Goyal MK, Gupta AK, Jha S, Das J, Madramootoo CA (2021) Joint behaviour of climate extremes across India: past and future. J Hydrol 597:126185

Kundu S, Khare D, Mondal A (2017) Future changes in rainfall, temperature and reference evapotranspiration in the central India by least square support vector machine. Geosci Front 8(3):583–596

Lambin EF, Meyfroidt P (2011) Global land use change, economic globalization, and the looming land scarcity. Proc Natl Acad Sci 108(9):3465–3472

Lewis SC, Karoly DJ (2013) Evaluation of historical diurnal temperature range trends in CMIP5 models. J Clim 26(22):9077–9089

Lindvall J, Svensson G (2015) The diurnal temperature range in the CMIP5 models. Clim Dyn 44(1–2):405–421

Lobell DB, Bonfils C, Duffy PB (2007) Climate change uncertainty for daily minimum and maximum temperatures: a model inter-comparison. Geophys Res Lett 34(5)

Mall RK, Singh N, Singh KK, Sonkar G, Gupta A (2018) Evaluating the performance of RegCM4.0 climate model for climate change impact assessment on wheat and rice crop in diverse agro-climatic zones of Uttar Pradesh, India. Clim Change 149(3):503–515

Mall RK, Srivastava RK, Banerjee T, Mishra OP, Bhatt D, Sonkar G (2019) Disaster risk reduction including climate change adaptation over south Asia: challenges and ways forward. Int J Disaster Risk Sci 10:14–27. https://doi.org/10.1007/s13753-018-0210-9

Mall RK, Chaturvedi M, Singh N, Bhatla R, Singh RS, Gupta A, Niyogi D (2021) Evidence of asymmetric change in diurnal temperature range in recent decades over different agro-climatic zones of India. Int J Climatol 41(4):2597–2610

McNider, R. T., Steeneveld, G. J., Holtslag, A. A. M., Pielke Sr, R. A., Mackaro, S., Pour-Biazar, A., ... & Christy, J. (2012). Response and sensitivity of the nocturnal boundary layer over land to added longwave radiative forcing. *Journal of Geophysical Research: Atmospheres*, *117*(D14).

Patel S, Mall RK, Jaiswal R, Singh R, Chand R (2022) Vulnerability assessment of wheat yield under warming climate in Northern India using multi-model projections. International Journal of Plant Production 16(4):611–626. https://doi.org/10.1007/s42106-022-00208-1

Pereira HM, Leadley PW, Proença V, Alkemade R, Scharlemann JP, Fernandez-Manjarrés JF, ..., Walpole M (2010) Scenarios for global biodiversity in the 21st century. Science 330(6010):1496–1501

Piao S, Friedlingstein P, Ciais P, de Noblet-Ducoudré N, Labat D, Zaehle S (2007) Changes in climate and land use have a larger direct impact than rising CO2 on global river runoff trends. Proc Natl Acad Sci 104(39):15242–15247

Pielke Sr RA, Marland G, Betts RA, Chase TN, Eastman JL, Niles JO, ..., Running SW (2002) The influence of land-use change and landscape dynamics on the climate system: relevance to climate-change policy beyond the radiative effect of greenhouse gases. Philosophical Transactions of the Royal Society of London. Ser A: Math Phys Eng Sci 360(1797):1705–1719

Pitman AJ, de Noblet-Ducoudré N, Cruz FT, Davin EL, Bonan GB, Brovkin V, ..., Voldoire A (2009) Uncertainties in climate responses to past land cover change: first results from the LUCID intercomparison study. Geophys Res Lett 36(14)

Pongratz J, Reick CH, Raddatz T, Claussen M (2010) Biogeophysical versus biogeochemical climate response to historical anthropogenic land cover change. Geophys Res Lett 37(8)

Praveen D, Andimuthu R, Parthasarathy R, Perumal T (2016) A preliminary assessment of observed and projected trends in the diurnal temperature ranges over South India under SRES A1B scenario. Int J Global Warming 9(1):1

Rajbhandari R, Shrestha AB, Kulkarni A, Patwardhan SK, Bajracharya SR (2015) Projected changes in climate over the Indus river basin using a high resolution regional climate model (PRECIS). Clim Dyn 44(1):339–357

Rajbhandari R, Shrestha AB, Nepal S, Wahid S (2016) Projection of future climate over the Koshi River basin based on CMIP5 GCMs. Atmos Clim Sci 6(2):190–204

Rajput P, Singh S, Singh TB, Mall RK (2023) The nexus between climate change and public health: a global overview with perspectives for Indian cities. Arab J Geosci 16(1):15. https://doi.org/10.1007/s12517-022-11099-x

Ruosteenoja K, Räisänen P, Devraj S, Garud SS, Lindfors AV (2019) Future changes in incident surface solar radiation and contributing factors in India in CMIP5 climate model simulations. J Appl Meteorol Climatol 58(1):19–35

Sala OE, Stuart Chapin FIII, Armesto JJ, Berlow E, Bloomfield J, Dirzo R, ..., Wall DH (2000). Global biodiversity scenarios for the year 2100. Science 287(5459):1770–1774

Salehnia N, Salehnia N, Torshizi AS, Kolsoumi S (2020) Rainfed wheat (Triticum aestivum L.) yield prediction using economical, meteorological, and drought indicators through pooled panel data and statistical downscaling. Ecol Indic 111:105991

Sanjay J, Krishnan R, Shrestha AB, Rajbhandari R, Ren GY (2017) Downscaled climate change projections for the Hindu Kush Himalayan region using CORDEX South Asia regional climate models. Adv Clim Chang Res 8(3):185–198

Sharma A, Goyal MK (2020) Assessment of drought trend and variability in India using wavelet transform. Hydrol Sci J 65(9):1539–1554

Shevliakova E, Pacala SW, Malyshev S, Hurtt GC, Milly PCD, Caspersen J, ..., Crevoisier C (2009) Carbon cycling under 300 years of land-use changes in the dynamic land model LM3V. Glob Biogeochem Cycles 23:GB2022

Sillmann J, Kharin VV, Zhang X, Zwiers FW, Bronaugh D (2013) Climate extremes indices in the CMIP5 multimodel ensemble: part 1. Model evaluation in the present climate. J Geophys Res: Atmos 118(4):1716–1733

Singh N, Banerjee T, Raju MP, Deboudt K, Sorek-Hamer M, Singh RS, Mall RK (2018) Aerosol chemistry, transport, and climatic implications during extreme biomass burning emissions over the Indo-Gangetic Plain. Atmos Chem Phys 18(19):14197–14215

Singh N, Mhawish A, Ghosh S, Banerjee T, Mall RK (2019) Attributing mortality from temperature extremes: a time series analysis in Varanasi, India. Sci Total Environ 665:453–464

Singh N, Mall RK, Banerjee T, Gupta A (2021a) Association between climate and infectious diseases among children in Varanasi city, India: a prospective cohort study. Sci Total Environ 796:148769

Singh S, Mall RK, Singh N (2021b) Changing spatio-temporal trends of heat wave and severe heat wave events over India: an emerging health hazard. Int J Climatol 41:E1831–E1845

Singh N, Mhawish A, Banerjee T, Ghosh S, Singh RS, Mall RK (2021c) Association of aerosols, trace gases and black carbon with mortality in an urban pollution hotspot over central Indo-Gangetic Plain. Atmos Environ 246:118088

Singh S, Mall RK, Dadich J, Verma S, Singh JV, Gupta A (2021) Evaluation of CORDEX-South Asia regional climate models for heat wave simulations over India. Atmos Res 248:105228. https://doi.org/10.1016/j.atmosres.2020.105228

Soni VK, Pandithurai G, Pai DS (2012) Evaluation of long-term changes of solar radiation in India. Int J Climatol 32(4):540–551

Sonkar G, Mall RK, Banerjee T, Singh N, Kumar TL, Chand R (2019) Vulnerability of Indian wheat against rising temperature and aerosols. Environ Pollut 254:112946

Sonkar G, Singh N, Mall RK, Singh KK, Gupta A (2020) Simulating the impacts of climate change on sugarcane in diverse agro-climatic zones of northern India using CANEGRO-sugarcane model. Sugar Tech 22:460–472. https://doi.org/10.1007/s12355-019-00787-w

Stone DA, Weaver AJ (2002) Daily maximum and minimum temperature trends in a climate model. Geophys Res Lett 29(9):70–71

Sun X, Ren G, You Q, Ren Y, Xu W, Xue X, ..., Zhang P (2019) Global diurnal temperature range (DTR) changes since 1901. Clim Dyn 52(5):3343–3356

Ullah A, Salehnia N, Kolsoumi S, Ahmad A, Khaliq T (2018) Prediction of effective climate change indicators using statistical downscaling approach and impact assessment on pearl millet (Pennisetum glaucum L.) yield through genetic algorithm in Punjab, Pakistan. Ecol Indic 90:569–576

Vinnarasi R, Dhanya CT, Chakravorty A et al (2017) Unravelling diurnal asymmetry of surface temperature in different climate zones. Sci Rep 7:7350. https://doi.org/10.1038/s41598-017-07627-5

Vose RS, Easterling DR, Gleason B (2005) Maximum and minimum temperature trends for the globe: an update through 2004. Geophys Res Lett 32(23)

Wahiduzzaman M, Yeasmin A (2020) A kernel density estimation approach of North Indian Ocean tropical cyclone formation and the association with convective available potential energy and equivalent potential temperature. Meteorol Atmos Phys 132(5):603–612

Wang F, Zhang C, Peng Y, Zhou H (2014) Diurnal temperature range variation and its causes in a semiarid region from 1957 to 2006. Int J Climatol 34(2):343–354

Waqas A, Athar H (2018) Observed diurnal temperature range variations and its association with observed cloud cover in northern Pakistan. Int J Climatol 38(8):3323–3336

Wild M (2009) How well do IPCC-AR4/CMIP3 climate models simulate global dimming/brightening and twentieth-century daytime and nighttime warming? J Geophys Res: Atmos 114(D10)

Wiltshire AJ (2014) Climate change implications for the glaciers of the Hindu Kush Karakoram and Himalayan region. Cryosphere 8(3):941–958

Zhou L, Dickinson RE, Dai A, Dirmeyer P (2010) Detection and attribution of anthropogenic forcing to diurnal temperature range changes from 1950 to 1999: comparing multi-model simulations with observations. Clim Dyn 35(7–8):1289–1307

Zhou L, Dickinson RE, Tian Y, Fang J, Li Q, Kaufmann RK, ..., Myneni RB (2004) Evidence for a significant urbanization effect on climate in China. Proc Natl Acad Sci 101(26):9540–9544

Zhuang Y, Zhang J (2020) Diurnal asymmetry in future temperature changes over the main Belt and Road regions. Ecosyst Health Sustain 6(1):1749530